Nanoscale

PAPER

View Article Online
View Journal | View Issue

Cite this: *Nanoscale*, 2018, **10**, 2045

High-*Q* and highly reproducible microdisks and microlasers†

Nan Zhang,‡[a] Yujie Wang,‡[a] Wenzhao Sun,[a] Shuai Liu,[a] Can Huang,[a] Xiaoshun Jiang,*[b] Min Xiao,*[b] Shumin Xiao*[a,c] and Qinghai Song *[a,c]

Received 17th November 2017,
Accepted 20th December 2017

DOI: 10.1039/c7nr08600h

rsc.li/nanoscale

High quality (*Q*) factor microdisks are fundamental building blocks of on-chip integrated photonic circuits and biological sensors. The resonant modes in microdisks circulate near their boundaries, making their performances strongly dependent upon surface roughness. Surface-tension-induced microspheres and microtoroids are superior to other dielectric microdisks when comparing *Q* factors. However, most photonic materials such as silicon and negative photoresists are hard to be reflowed and thus the realizations of high-*Q* microdisks are strongly dependent on electron-beam lithography. Herein, we demonstrate a robust, cost-effective, and highly reproducible technique to fabricate ultrahigh-*Q* microdisks. By using silica microtoroids as masks, we have successfully replicated their ultrasmooth boundaries in a photoresist *via* anisotropic dry etching. The experimentally recorded *Q* factors of passive microdisks can be as large as 1.5×10^6. Similarly, ultrahigh *Q* microdisk lasers have also been replicated in dye-doped polymeric films. The laser linewidth is only 8 pm, which is limited by the spectrometer and is much narrower than that in previous reports. Meanwhile, high-*Q* deformed microdisks have also been fabricated by controlling the shape of microtoroids, making the internal ray dynamics and external directional laser emissions controllable. Interestingly, this technique also applies to other materials. Silicon microdisks with $Q > 10^6$ have been experimentally demonstrated with a similar process. We believe this research will be important for the advances of high-*Q* micro-resonators and their applications.

Introduction

Optical microcavities have been intensively studied in the past decades due to their practical applications in on-chip photonic networks,[1–4] quantum information,[5–7] and environmental monitoring.[8–10] Whispering-gallery-mode (WGM) based optical microcavities are prominent examples. In general, electromagnetic waves with specific frequencies are confined by total internal reflection and circulate along the cavity perimeter for a long time. The peak powers of the circulating waves can be orders of magnitude higher than the incident light and thus the nonlinearity, light–matter interaction, and detection sensitivity in WGM microcavities have been significantly improved.[11,12] To date, *Q* factors of more than 100 million are attainable in silica based microtoroids and microspheres, whose surface roughness was smoothed to an atomic level by the reflow process,[13–15] while such kinds of high-*Q* resonators have paved new routes to ultra-wideband frequency combs,[16,17] green photonic devices,[18–20] and single nanoparticle or molecule detection.[9,21–24] The low refractive index of silica and its relatively poor resistance to acid and alkaline solutions strongly hinders its practical application, especially in environmental monitoring.[21] Meanwhile, the reflow temperature of silica is too high for functional materials such as organic molecules and quantum dots and thus its applications in functional devices are limited.[9,25]

The above limitations have the possibility to be solved using cross-linked polymers.[24,25] The refractive index of cross-linked polymers at telecommunication wavelengths can be much larger than 1.5. Some cross-linked polymers have large hardness and a high glass transition temperature, and they can withstand most standard acidic and alkaline plating solutions, as well as a strong alkaline solution with a pH of 13 at a high temperature.[26,27] These unique properties make the cross-linked polymers very attractive for applications in low-loss polymeric photonic devices, especially for some extreme

[a]*State Key Laboratory on Tunable Laser Technology, Ministry of Industry and Information Technology Key Lab of Micro-Nano Optoelectronic Information System, Shenzhen Graduate School, Harbin Institute of Technology, Shenzhen, 518055, China. E-mail: shumin.xiao@hit.edu.cn, qinghai.song@hit.edu.cn*
[b]*National Laboratory of Solid State Microstructures and College of Engineering and Applied Sciences, Nanjing University, Nanjing 210093, China. E-mail: jxs@nju.edu.cn, minxiao@nju.edu.cn*
[c]*Collaborative Innovation Center of Extreme Optics, Shanxi University, Taiyuan 030006, China*

†Electronic supplementary information (ESI) available. See DOI: 10.1039/c7nr08600h

‡These two authors contributed equally to this work.

conditions.[28,29] In past decades, several fabrication protocols have been developed to produce high-Q polymeric microdisks, *e.g.* replica molding[30] and thermal-reflow methods with surface-tension induced cavity geometries.[31] While the surface roughness has been significantly improved, their Q factors are still limited by surface scattering. Meanwhile, the cavity shapes are restricted to microtoroids and their thicknesses cannot be precisely controlled. Very recently, two-photon polymerization,[32,33] laser direct writing,[34,35] and electron-beam lithography[36] have been applied to produce polymeric microdisks on both the glass substrate and the silicon substrate. Based on these technologies, microdisks with Q factors above 10^6 have been successfully generated.[36] However, due to the fabrication deviation, the resonant wavelengths of such high-Q microdisks are hard to be reproduced and these methods are not applicable to inorganic materials such as silicon, silicon nitride, *etc.* In this research, we experimentally demonstrate a robust and effective technique to fabricate ultrahigh-Q and highly reproducible microdisks in polymer films and SOI wafers.

Results and discussion

In principle, the Q factor of a micro-resonator can be expressed as $1/Q = 1/Q_r + 1/Q_{ss} + 1/Q_a$, where Q_r, Q_{ss}, and Q_a are related to optical loss due to radiation, surface scattering, and absorption of materials, respectively.[37] In WGM microcavities, the light is confined with total internal reflection and the radiation loss is usually orders of magnitude smaller than the others. In this sense, an ultra-smooth surface and ultralow material loss are two fundamental criteria to realize high-Q microdisks. In this experiment, we select the epoxy novolac resin (ENR) photoresist (SU8) to fabricate high-Q microdisks. In addition to its better hardness, higher glass transition temperature, and higher refractive index, the material loss of the SU8 photoresist at telecommunication wavelengths is much lower than that of PMMA. In an ENR waveguide with surface roughness, the propagation loss can be as low as 0.48 dB cm^{-1} at 1550 nm, which ensures relatively high Q factors if the surface roughness of SU8 microdisks is improved.

Fabrication and characterization of passive SU8 microdisks

Different from the electron-beam resists such as PMMA and ZEP, the SU8 photoresist can accumulate charges and it is hard to be reflowed. Thus high-Q SU8 microdisks cannot be fabricated with conventional methods, *e.g.* electron-beam lithography and thermal reflow.[26–36] To improve the surface roughness and to avoid the toroidal device shape, we have developed a new technique that can replicate the smooth boundary of microtoroids in designed materials. Fig. 1 illustrates the schematic picture of the fabrication process. The whole experiment starts with ultrahigh-Q silica microtoroids that are fabricated with a combination of standard photolithography, dry etching and a selective reflow process.[13] The major diameters of the microtoroids range from 50 to 60 μm, with minor diameters from 4 to 6 μm. Inset-I in Fig. 1 shows the top-view scanning electron microscope (SEM) image of one silica microtoroid. Owing to the reflow process, the surface roughness of the silica microtoroids is negligibly small. The optical characteristics of the microtoroids have been thoroughly studied in the past decade. High Q factors above 100 million have been successfully obtained.

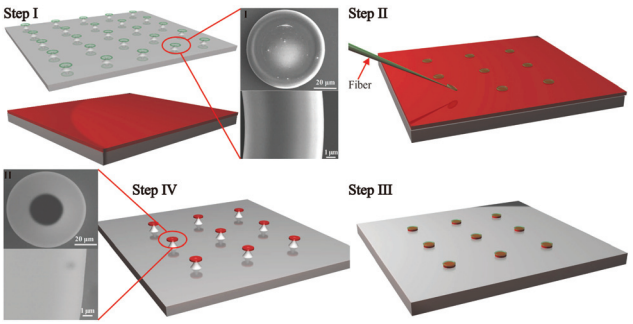

Fig. 1 Schematic picture of the fabrication process of a high-Q SU8 microdisk. Inset-I is the top-view SEM image and the high resolution SEM image of an initial silica microtoroid. Inset-II shows the top-view SEM image and the high resolution SEM image of the fabricated SU8 microdisk.

The fabricated microtoroids are removed from their initial substrate and transferred to an SU8 coated silicon wafer with a tapered fiber. The SU8 film is spin-coated onto a silicon wafer and is cross-linked after curing with UV light and hard baked at 170 degrees for an hour. The thickness of the SU8 film is around 1.9 μm, which is controlled by the spin-coating speed. Then polymeric microdisks are fabricated by two steps of ICP etching. In the first step, the sample is anisotropically etched by O_2 in ICP for 3 minutes at 20 °C (the flow rate of O_2 and the pressure of the chamber are 10 sccm and 2 mTorr, respectively, whereas the RF power and the ICP power are 120 Watt and 400 Watt, respectively). As SiO_2 cannot be etched by oxygen, the microtoroids functioned as masks and their shapes were well replicated in the SU8 photoresist by anisotropic etching. After the first etching step, the SiO_2 microtoroids have been removed to another silicon wafer for further experiment (see below). Then the whole wafer was etched again with SF_6 in ICP. As reported earlier, the silicon substrate should be isotopically etched in this process and pedestals could be formed underneath the microdisk to well separate it from the substrate.[38] In this experiment, the diameters of pedestals are around 25 microns, which is small enough to exclude their influence on the high-Q resonance microdisks, and study their lasing actions.

Inset-II in Fig. 1 shows the top-view SEM image of the SU8 microdisk. Both the shape and the surface roughness of the of the SU8 microdisk inherit the microtoroid well. Even in the high resolution SEM image, the surface roughness is still very small and hard to be resolved. Considering the high Q factor of the SiO_2 microtoroids, this kind of surface roughness can ensure high Q factors of polymeric microdisks. The differences between the SU8 microdisk and the SiO_2 microtoroid

mask lie in the vertical direction. Different from the replica modelling in previous reports, here the microdisk inherits only the in-plane boundary shape of the microtoroid. Its thickness is determined by the thickness of the SU8 film instead of the minor diameter of the microtoroid. Consequently, the polymeric microdisk does not have toroidal parts and can be considered as a smooth waveguide in the vertical direction. This kind of cavity shape is good for fundamental studies on ray and wave correspondence, quantum chaos, and dynamical tunnelling.

Then the Q factors of the polymeric microdisks are examined. The polymeric microdisks are mounted onto a high-resolution translation stage (100 nm step resolution) and monitored by cameras. The input light is coupled to the polymeric microdisks *via* the evanescent coupling through a tapered fiber and the transmittance is measured at the throughput port. By scanning the wavelength of the input laser (linewidth of 100 kHz), the resonances in polymeric microdisks can be clearly seen from the transmission dips in the spectrum. One example is shown in Fig. 2. For a microdisk with a diameter of ~65 μm, a series of periodic resonances can be clearly seen. The free spectral range of the SU8 microdisk is around 4.8 nm (see Fig. S11 in the ESI†). Considering the cavity size and the refractive index of SU8, these modes correspond to high Q resonances along the boundary of the polymeric microdisk well. Fig. 2(b) shows the high resolution spectrum of one resonance. As the input power and the laser scan frequency have been optimized, the effect of thermal distortion is minimized and the obtained resonant dip can be fitted to a Lorentzian shape. The fitted full width at half maximum (FWHM) is around 1 pm, giving a Q factor around 1.5×10^6. This value is much higher than the microdisks that are fabricated with electron beam lithography and two-photon polymerization.[32–36] Therefore, we know that high-Q polymeric microdisks can be simply formed by combining SiO_2 microtoroids as masks and anisotropic ICP etching.

WGM lasers in dye-doped SU8 microdisks

Owing to the unique properties of polymers, many functional materials can be simply doped inside to realize particular functions such as nonlinear optics, optical switches, lasers, and modulators.[28,29] Since the above fabrication process is totally operated at room temperature, functional materials can also be doped inside the microdisks. To validate this potential, we have doped Rhodamine B into the SU8 photoresist and tested its applications on polymeric microdisks in lasers. The dye molecules were directly dissolved in the photoresist solution with 8% weight.[39] With a similar process as above, active microdisks have been successfully fabricated. Fig. 3(a) shows the top-view SEM image of one polymeric microdisk. While dye molecules have been doped, the cavity boundary shapes are still very smooth and no obvious surface roughness can be seen. The tilt-view SEM image with larger magnification is shown in Fig. S3† in section 2 of the ESI†. No obvious surface roughness can be seen even though the scale bar is increased to 100 nm. In this sense, these dye-doped microdisks can also have relatively high Q factors and narrow linewidth microdisk lasers can be expected.

To characterize their optical properties, the dye-doped microdisks are optically excited with a frequency doubled Nd:YAG nanosecond laser (532 nm, repetition rate 10 Hz, pulse duration 7 ns). Basically, the dye-doped microdisks are placed onto a rotational translation stage under a home-made optical microscope. The pumping laser is focused by an objective lens onto the top surface of the microdisk in the normal direction. The focus point is around 50 microns in diameter to cover the whole microdisk. As the microdisks mainly have in-plane emissions, the outputs from microdisks are collected by an optical lens at the side (see section 2 of the ESI†) and transported to a spectrometer *via* a multimode fiber. A polarizer is placed between the lens and fiber to test the polarization. Fig. 3(b) shows the emission spectra from the SU8 microdisk at different pumping powers. When the pumping power is low, the emission is a broad photoluminescence peak. Once the pumping power is increased to 0.29 μJ, sharp laser peaks

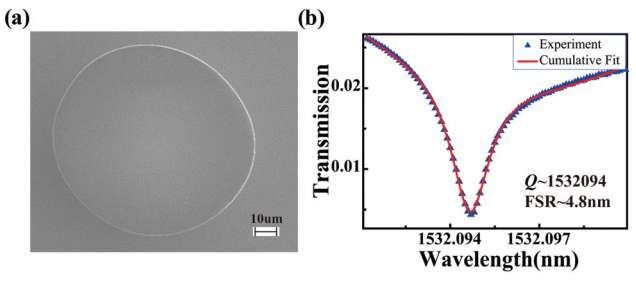

Fig. 2 A high Q passive polymeric WGM microdisk. (a) The transmission spectrum for a 65 μm diameter SU8 microdisk. (b) The high resolution spectrum of resonance at 1550 nm. The full width at half maximum is only 1 pm, giving a Q factor around 1.5×10^6.

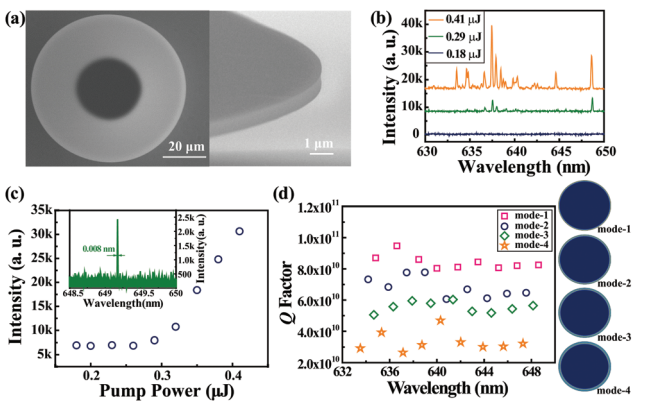

Fig. 3 A high Q active polymeric WGM microdisk. (a) The top-view and side-view SEM image of a dye-doped SU8 microdisk taken at 45 degrees. (b) The emission spectra of dye-doped SU8 microdisks under different pumping densities. (c) The output intensity as a function of pumping density. The inset shows the high resolution spectrum of one laser mode. The corresponding linewidth is as small as ~0.008 nm. (d) The numerically calculated Q factors of resonant modes and the simulated field pattern.

emerge at around 637 nm and 649 nm, respectively. Further increasing the pumping power, more discrete laser peaks have been observed and these sharp peaks rapidly dominated the emission spectra. The dots shown in Fig. 3(c) summarize the integrated intensity of the emission spectrum as a function of pumping power. Associated with the emergence of sharp peaks, the integrated output intensity also increases dramatically with the pumping power, clearly demonstrating the threshold behaviors at ~0.29 μJ.

The inset in Fig. 3(c) shows the high resolution spectrum of a microdisk laser at the threshold. The fitted FWHM of the laser peak is as narrow as 8 pm. As this linewidth approaches the resolution limit of our spectrometer, we repeated the optical measurement several times to exclude the possibility of noise. Based on the narrow linewidth, the Q factor of the microdisk laser can be simply estimated as $Q = \lambda/\Delta\lambda = 0.8 \times 10^5$. While this Q factor is limited by the spectral resolution and lower than the result shown in Fig. 2, it is already much higher than the previous reports on polymer lasers.[28,29,31,34,39] As mentioned above, this kind of high Q factors benefit from the ultra-smooth cavity boundaries of polymeric microdisks (see inset-II in Fig. 1).

In addition to the linewidth, the ultra-smooth cavity boundary of the microdisk laser can also be confirmed from the mode number. In principle, both the radiation loss and the scattering loss are much smaller; the Q values of polymeric microdisks are determined by the material loss. In this sense, WGMs with different radial numbers should have quite close Q factors (Q_{abs}) and can be excited simultaneously. This phenomenon has been indeed observed in our experiment. As shown in Fig. 3(b), a large number of lasing modes have been experimentally observed. For a microdisk with diameter ~78 μm, the free spectral range of the dye-doped SU8 microdisk is around 1.7 nm. Following the numerical calculation of WGMs, these lasing modes can be categorized into several groups with different radial numbers (see Fig. 3(b) and (d)). As a control experiment, we have fabricated circular microdisks with standard photolithography. In these relatively rough microdisks, only one to two sets of WGMs can be excited (see Fig. S4 in the ESI†).[29] Therefore, both the laser spectra and the ultra-narrow linewidths demonstrate that high-Q microdisk lasers have been successfully replicated from microtoroids *via* the anisotropic ICP etching.

Directional laser emissions in dye-doped SU8 microdisks

Different from the initial microtoroid, the polymeric microdisk is uniform in the third direction and won't have additional coupling in and coupling out loss between the toroidal parts and the internal disk. Consequently, the replicated polymeric microdisks can also function as platforms to study the ray dynamics.[40–43] Here we take a deformed limaçon microdisk as a sample to illustrate these applications. Following the above fabrication process, the dye-doped SU8 microdisks have been fabricated. The only difference that occurred was in controlling the boundary shape of the microtoroids, which has been reported by Jiang *et al.*[44] Fig. 4(a) shows the top-view SEM image of the microdisk. The boundary shape can be fitted to a limaçon cavity, which is defined as $\rho(\theta) = R(1 + 0.43\cos\theta)$ in polar coordinates. Here R is 40 μm and the thickness of the microdisk is also maintained at 1.9 μm.[42,45]

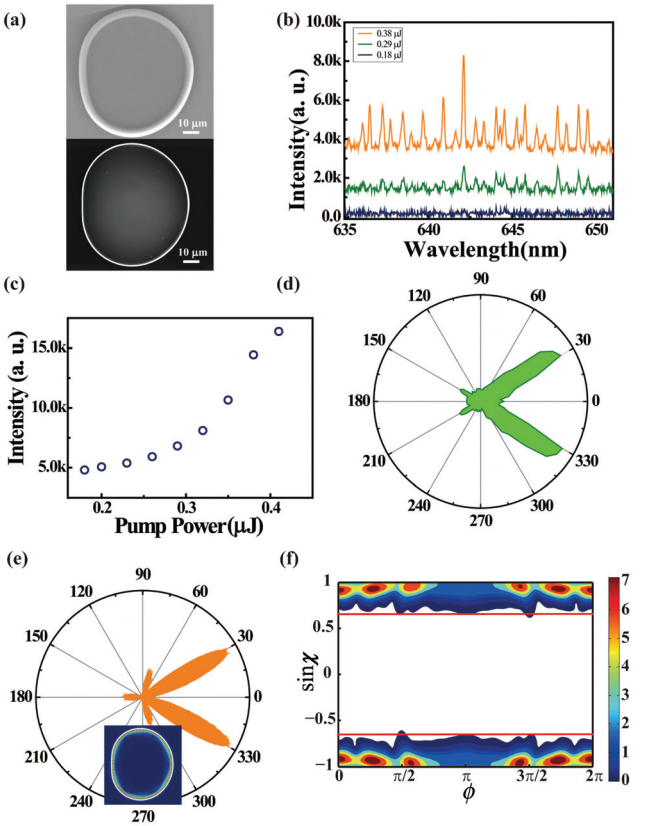

Fig. 4 The confirmation of chirality. (a) and (c) are the top-view SEM images of the waveguide coupled limaçon-spiral photonic molecule and a single limaçon microdisk. (b) and (d) are their corresponding fluorescent microscope images above laser thresholds.

Then the optical characteristics of the deformed microdisk are examined by optical excitation. Similar to the circular disk, the emission of the deformed microdisk is still a broad photoluminescence peak at a low pumping density. With the increase of pumping power, sharp peaks emerge and finally dominate the emission spectrum. The dependence of output intensity on the pumping power has also been recorded. As shown in Fig. 4(c), an obvious laser threshold can be observed at around 0.3 μJ. While these behaviors are very close to the results shown in Fig. 3, the lasing actions in the deformed limaçon microdisk are totally different. In a deformed limaçon microdisk, the large deformation in cavity boundary makes the ray dynamics almost completely chaotic (see the Fig. S16 in the ESI†). In a chaotic microcavity, the WGMs with different radial numbers cannot exist anymore. While high Q resonances can still be trapped near the cavity boundary, they are confined by wave localization along the chaotic orbits at large $\sin\chi$ instead of WGM orbits.[45] Consequently, only one or two sets of resonances can have relatively high Q factors and the

laser spectra are much simpler. This is indeed what we have observed. As shown in Fig. 4(b), the deformed microdisk has only one set of lasing modes, whose free spectral range matches the chaotic modes confined by the wave localization well (see section 3.2 of the ESI†). The linewidth of the microdisk laser at threshold is as narrow as 0.014 nm.

In addition to the light confinement, the chaotic motions can also dramatically affect the laser emission. In a circular microdisk, the light is confined by total internal reflection. The corresponding laser emissions are isotropic. In a chaotic microcavity, the light usually propagates along the cavity boundary for a while and then quickly transmits out following the unstable manifolds.[46] In this sense, the deformed microdisks usually produce directional laser emissions that are important for practical applications.[28] For the replicated deformed limaçon microdisk, its far field pattern has also been experimentally studied by rotating the translation stage. The experimental results are summarized in Fig. 4(d), where two directional laser beams along $\phi_{FF} = \pm 60^{\circ}$ can be clearly seen. In order to understand the lasing actions, we have also numerically studied the resonances in limaçon microdisks. Similar to experimental observations, a series of high Q resonances have been seen. By projecting the wave function along the cavity boundaries into phase space, the phase space structures of these modes have been studied.[47] One example is illustrated in Fig. 4(f), similar to the above analysis; the waves are well confirmed at large $\sin\chi$ and decay to critical lines following the unstable manifolds. The CCW waves ($\sin\chi > 0$) directly transmit out at $\theta \sim 3\pi/2$. Similarly, the CW waves leak at $\theta \sim \pi/2$. Since the CW components and the CCW components are balanced in the limaçon cavity (see Fig. 4(f)), two symmetric laser beams can thus be seen in Fig. 4(e). This far field pattern is exactly what we have experimentally observed and thus confirmed the internal ray dynamics very well.

The reproducibility of polymeric microdisks

Due to unavoidable fabrication deviation, the reproducibility of microdisks is always a severe challenge. In our method, because the oxygen plasma cannot etch the SiO_2, the cavity shape and surface roughness of SiO_2 microtoroids can be well preserved. In this sense, the toroidal masks are reusable and polymeric microdisks with the same resonant properties are possibly generated. One example is illustrated in Fig. 5. By using the same microtoroid, four SU8 microdisks have been fabricated in sequence. Following their chronological order, these microdisks have been numbered as disk-1 to disk-4. The resonant properties of these microdisks have been optically characterized by measuring their lasing spectra *via* optical pumping. We can see that the resonant frequencies, linewidths, and peak numbers are all the same in the four microdisks, clearly demonstrating the great potential of our technique in fabricating highly reproducible microdisks.

The extension to silicon microdisks

In addition to the advantages in fabricating high Q, reproducible polymer microdisks, this method can also be extended to other materials. Here we take silicon as an example to demonstrate this possibility. The typical process for the fabrication of high Q silicon microdisks consists of electron beam lithography, thermal reflow, and anisotropic ICP etching. This method requires considerable cost and time. Here we show that the combination of a microtoroid template and ICP etching can release the dependence on electron beam lithography. Similar to the fabrication process in polymeric microdisks, we transferred the SiO_2 microtoroids onto a silicon on insulator (SOI) wafer. The thicknesses of the silicon layer and insulator are 220 nm and 3 μm, respectively. After placing the microtoroids, the SOI wafer was placed in ICP and etched with SF_6 and C_4F_8. As the reaction between Si and C_4F_8 can form a protective layer in the horizontal direction, the etching process is quite anisotropic and thus the cavity boundary of the microtoroids can be replicated in the silicon layer. The silicon microdisk was finally achieved by selectively etching the SiO_2 present underneath with diluted HF at room temperature.

Fig. 6(a) shows the top-view SEM image of the silicon microdisk. The corresponding high resolution SEM image shows that the silicon microdisk is extremely smooth and no obvious roughness can be observed. According to previous reports, high Q factors above 10^6 can be expected. Similar to Fig. 2, we have also studied the resonant properties by measuring the transmission spectrum. Fig. 6(b) shows one transmission dip

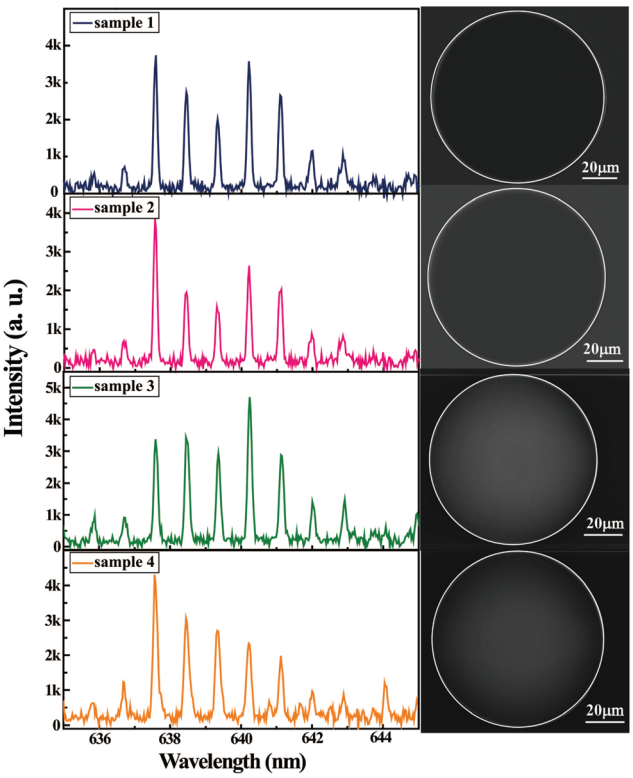

Fig. 5 The reproducibility of SU8 microdisk lasers. The laser spectra of active SU8 microdisks that are individually etched with the same microtoroid mask. The corresponding top-view SEM images are plotted as insets.

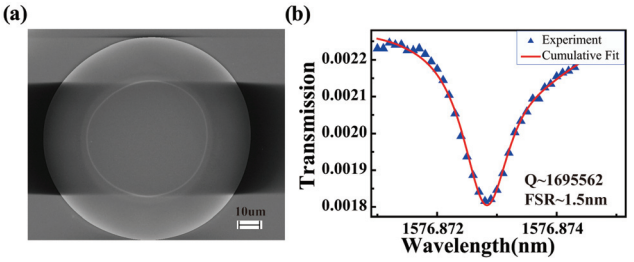

Fig. 6 The realization of a high-Q silicon microdisk. (a) The top-view SEM image and the high resolution SEM image of a silicon microdisk. (b) The transmission spectrum of the silicon microdisk.

of the WGM. As the laser power and the scanning speed have been optimized, here the transmission dip can also be fitted to a Lorentzian shape. The fitted linewidth is around 0.0009 nm, giving a Q factor more than 1.7×10^6. The free spectral range of the silicon microdisk is around 1.5 nm (see Fig. S12 in the ESI†). While no high-cost electron beam lithography has been employed in this method, the obtained Q factor is still close to the record high Q value of the silicon microdisk.[38] Similar to the polymeric microdisk, this method can also be applied to fabricate deformed microdisks.

Conclusions

In summary, we have developed a robust, cost-effective, and highly reproducible method to fabricate ultrahigh-Q microdisks. By using silica microtoroids with atomically smooth boundaries as templates, their ultrasmooth boundaries have been successfully replicated within the photoresist *via* anisotropic dry etching. The experimentally recorded Q factors can be larger than 10^6, which are limited by material absorption. By doping dye molecules, microdisk lasers with ultra-narrow linewidth have also been demonstrated. The experimentally recorded linewidth is only 8 pm, which is a record value in polymeric microlasers. Meanwhile, as the replicated microdisk is uniform in the third direction, the polymeric microdisks have also been applied to study the ray dynamics in microsystems. By deforming the microdisk from a circle to a limaçon, we have also observed directional laser emissions with narrow linewidth from the replicated polymer microdisk. Interestingly, the developed technique is not limited to polymers. It also applies to other materials and high-Q silicon microdisks on a SOI wafer have been experimentally demonstrated with a similar process. This research will be important for the advances of high-Q micro-resonators and their applications, especially for some materials that have very low selectivity to conventional photoresists and electron-beam resists.

Conflicts of interest

There are no conflicts to declare.

Acknowledgements

The author would like to thank the financial support from the Shenzhen Fundamental research projects under grant no. JCYJ20160427183259083, the Public platform for fabrication and detection of micro- & nano-sized aerospace devices, and the Shenzhen engineering laboratory on organic–inorganic perovskite devices. N. Zhang and Y. Wang contributed equally to this work.

Notes and references

1 R. Soref, *Silicon*, 2010, **2**, 1–6.
2 S. Feng, T. Lei, H. Chen, H. Cai, X. Luo and A. W. Poon, *Laser Photonics Rev.*, 2012, **6**, 145–177.
3 W. Bogaert, P. D. Heyn, T. V. Vaerenbergh, K. D. Vos, S. K. Selvaraja, *et al.*, *Laser Photonics Rev.*, 2012, **6**, 47–73.
4 L. Liu, R. Kumar, K. Huybrechts, T. Spuesens, G. Roelkens, *et al.*, *Nat. Photonics*, 2010, **4**, 182–187.
5 K. Nemoto, M. Trupke, S. J. Devitt, *et al.*, *Phys. Rev. X*, 2014, **4**, 031022.
6 F. J. Rodríguez-Fortuno, I. Barber-Sanz, D. Puerto, A. Griol and A. Martínez, *ACS Photonics*, 2014, **1**, 762–767.
7 M. Hafezi, S. Mittal, J. Fan, A. Migdall and J. M. Taylor, *Nat. Photonics*, 2013, **7**, 1001–1005.
8 J. Zhu, S. K. Ozdemir, Y. F. Xiao, L. Li, L. He, D. R. Chen and L. Yang, *Nat. Photonics*, 2010, **4**, 46–49.
9 A. M. Armani, R. P. Kulkami, S. E. Fraser, R. C. Flagan and K. J. Valaha, *Science*, 2007, **317**, 783–787.
10 H. K. Hunt and A. M. Armani, *Nanoscale*, 2010, **2**, 1544–1559.
11 K. J. Vahala, *Nature*, 2002, **424**, 839.
12 L. He, S. K. Ozdemir and L. Yang, *Laser Photonics Rev.*, 2013, **7**, 60–82.
13 D. K. Armani, T. J. Kippemberg, S. M. Spillane and K. J. Vahala, *Nature*, 2003, **421**, 925–928.
14 S. M. Spillane, T. J. Kippenberg, K. J. Vahala, K. W. Goh, E. Wilcut and H. J. Kimble, *Phys. Rev. A*, 2005, **71**, 013817.
15 L. Yang and K. J. Vahala, *Opt. Lett.*, 2003, **8**, 592–594.
16 T. J. Kippenberg, R. Holzwarth and S. A. Diddams, *Science*, 2011, **332**, 555–559.
17 P. D. Haye, O. Arcizet, A. Schliesser, R. Holzwarth and T. J. Kippenberg, *Phys. Rev. Lett.*, 2008, **101**, 053903.
18 F. Monifi, J. Friedlein, S. K. Ozdemir and L. Yang, *J. Lightwave Technol.*, 2012, **21**, 3306–3315.
19 T. Lu, L. Yang, R. V. Loon, A. Polman and K. J. Vahala, *Opt. Lett.*, 2009, **34**, 482–484.
20 L. Chang, X. Jiang, S. Hua, C. Yang, J. Wen, *et al.*, *Nat. Photonics*, 2014, **8**, 524–529.
21 F. Vollmer and L. Yang, *Nanophotonics*, 2012, **1**, 267–291.
22 F. Vollmer and S. Arnold, *Nat. Methods*, 2008, **5**, 591–596.
23 L. He, S. K. Ozdemir, J. Zhu, W. Kim and L. Yang, *Nat. Nanotechnol.*, 2011, **6**, 428–432.

24 L. Shao, X. F. Jiang, X. C. Yu, B. B. Li, W. R. Clements, *et al.*, *Adv. Mater.*, 2013, **25**, 5616–5620.
25 M. D. Baaske, M. R. Foreman and F. Vollmer, *Nat. Nanotechnol.*, 2014, **9**, 933–939.
26 C. H. Dong, L. He, Y. F. Xiao, V. R. Gaddam, S. K. Ozdemir, *et al.*, *Appl. Phys. Lett.*, 2009, **94**, 231119.
27 A. M. Armani, A. Srinivasan and K. J. Vahala, *Nano Lett.*, 2007, **7**, 1823–1826.
28 N. Zhang, Z. Y. Gu, S. Liu, Y. J. Wang, S. Wang, *et al.*, *Optica*, 2017, **9**, 1151–1156.
29 N. Zhang, Z. Y. Gu, K. Y. Wang, M. Li, L. Ge, *et al.*, *Laser Photonics Rev.*, 2017, **11**, 1700052.
30 A. L. Martin, D. K. Armani, L. Yang and K. J. Vahala, *Opt. Lett.*, 2004, **29**, 533–535.
31 T. Ling, S. L. Chen and L. Jay Guo, *Opt. Express*, 2011, **19**, 861–869.
32 H. B. Sun and S. Kawata, *Adv. Polym. Sci.*, 2004, **170**, 169–273.
33 X. Cheng, L. J. Guo and P. F. Fu, *Adv. Mater.*, 2005, **17**, 1419–1424.
34 M. K. Gonokami, R. H. Jordan, A. Dodabalapur, H. E. Katz, M. L. Schilling, R. E. Slusher and S. Ozawa, *Opt. Lett.*, 1995, **20**, 2093–2095.
35 Z. P. Liu, Y. Li, Y. F. Xiao, B. B. Li, X. F. Jiang, *et al.*, *Appl. Phys. Lett.*, 2010, **97**, 211105.
36 T. Grossmann, M. Hauser, T. Beck, C. Gohn-Kreuz, M. Karl, H. Kalt, C. Vannahme and T. Mappes, *Appl. Phys. Lett.*, 2010, **96**, 013303.
37 P. E. Barclay, K. Srinvasan and O. Painter, *Opt. Express*, 2005, **13**, 801–820.
38 Y. J. Wang, N. Zhang, Z. Q. Jiang, L. Wang, Y. F. Xiao, *et al.*, *Adv. Mater. Technol.*, 2017, **2**, 1600299.
39 M. Li, N. Zhang, K. Wang, J. Li, S. Xiao and Q. Song, *Sci. Rep.*, 2015, **5**, 13682.
40 J. U. Nockel and A. D. Stone, *Nature*, 1997, **385**, 45–47.
41 C. Gmachl, F. Capasso, E. E. Narimanov, J. U. Nockel, A. D. Stone, J. Faist, D. L. Sivco and Y. C. Alfred, *Sicence*, 1998, **280**, 1556–1564.
42 Q. Song, L. Ge, A. D. Stone, H. Cao, J. Wiersig, J.-B. Shim, J. Unterhinninghofen, W. Fang and G. S. Solomon, *Phys. Rev. Lett.*, 2010, **105**, 103902.
43 A. Backer, R. Ketzmerick, S. Lock, J. Wiersig and M. Hentschel, *Phys. Rev. A*, 2009, **79**, 063804.
44 X. F. Jiang, Y. F. Xiao, C. L. Zou, L. He, C. H. Dong, *et al.*, *Adv. Mater.*, 2012, **24**, OP260–OP264.
45 J. Wiersig and M. Hentschel, *Phys. Rev. Lett.*, 2008, **100**, 033901.
46 H. G. Schwefel, N. B. Rex, H. E. Tureci, R. K. Chang, A. D. Stone, T. Ben-Messaoud and J. Zyss, *J. Opt. Soc. Am. B*, 2004, **21**, 923–934.
47 M. Hentschel and H. Schomerus, *Europhys. Lett.*, 2003, **62**, 5.